Original Research Article

Reflection and Refraction Phenomena of Elastic Waves Propagating Through Imperfect Interface of Solids

M S Barak*, Vinod Kaliraman#

*Department of Mathematics, Indira Gandhi University, Meerpur (Rewari), INDIA.
#Department of Mathematics, Chaudhary Devi Lal University, Sirsa-125055, INDIA.
Email: ms_barak@rediffmail.com, vsisaiya@gmail.com

Abstract

In this paper, the reflection and transmission of plane waves from imperfect interface separating a micropolar viscoelastic solid half space and a fluid saturated incompressible porous solid half space is studied. A longitudinal wave (P-wave) or transverse wave (SV-wave) impinges obliquely at the interface. Amplitude ratios for various reflected and transmitted waves have been obtained with help of boundary conditions at the interface. Then these amplitude ratios have been computed numerically for a specific model and results thus obtained are shown graphically with angle of incidence of incident wave. It is found that these amplitude ratios depend on angle of incidence of the incident wave, imperfect interface as well as on the properties of media. From the present investigation, a special case when fluid saturated porous half space reduces to empty porous solid and micropolar viscoelastic solid half space reduces to micropolar elastic solid has also been deduced and discussed with the help of graphs.

Key Words: Micropolar viscoelastic solid, porous, reflection, transmission, longitudinal wave, transverse wave, amplitude ratios, empty porous solid.

***Address for Correspondence:**
Vinod Kaliraman, Department of Mathematics, Chaudhary Devi Lal University, Sirsa-125055, Haryana, INDIA.
Email: vsisaiya@gmail.com

Received Date: 21/10/2017 Revised Date: 17/11/2017 Accepted Date: 10/12/2017

Access this article online	
Quick Response Code:	Website: www.medpulse.in
	Accessed Date: 10 January 2018

INTRODUCTION

Most of natural and man-made materials, including engineering, geological and biological media, possess a microstructure. The ordinary classical theory of elasticity fails to describe the microstructure of the material. To overcome this problem, Suhubi and Eringen (1964), Eringen and Suhubi (1964) developed a theory in which they considered the microstructure of the material and they showed that the motion in a granular structure material is characterized not by a displacement vector but also by a rotation vector. Gautheir (1982) found aluminum-epoxy composite to be a micropolar material. Eringen (1967) developed the linear theory of micropolar viscoelasticity. Many researchers discussed the problems of waves and vibrations in micropolar viscoelastic solids. Based on the work of Fillunger model (1913), Bowen (1980) and de Boer and Ehlers (1990a, 1990b) developed an interesting theory for porous medium having all constituents to be incompressible. Based on this theory, many researchers like de Boer and Liu (1994, 1995), Liu (1999), Singh (2002), de Boer and Didwania (2004), Kumar and Barak (2007), Kumar and Hundal (2007), Kumar *et.al.* (2011) etc. studied some problems of wave propagation in fluid saturated incompressible porous media. Elastic waves propagation in fluid saturated porous media has its importance in various fields such as soil dynamics, hydrology, seismology, earthquake engineering and geophysics. Imperfect interface considered in this problem means that the stress components are continuous and small displacement field is not. The values of the interface parameters depend upon the material properties of the medium. Recently, using the imperfect conditions at the interface, Chen *et.al.* (2004), Kumar and Chawala (2010), Kumari (2014) etc. studied the various types of wave problems. Using the theory of de Boer and Ehlers (1990) for fluid saturated porous medium and Eringen (1967) for micro polar elastic solid, the reflection and transmission phenomenon

How to site this article: M S Barak, Vinod Kaliraman. Reflection and Refraction Phenomena of Elastic Waves Propagating Through Imperfect Interface of Solids. *International Journal of Statistika and Mathemtika*. August to October 2017; 24(1): 01-11.
http://www.statperson.com

of longitudinal and transverse waves at an imperfect interface between micropolar elastic solid half space and fluid saturated porous solid half space is studied. A special case when fluid saturated porous solid half space reduces to empty porous solid half space has been deduced and discussed. Amplitudes ratios for various reflected and transmitted waves are computed for a particular model and depicted with help of graphs and discussed accordingly. The model which is considered here is assumed to exist in the oceanic crust part of the earth and the propagation of wave through such a model will be of great use in the fields which are related to earth sciences.

BASIC EQUATIONS AND CONSTITUTIVE RELATIONS

For medium M_2 (Micropolar viscoelastic solid)

Following Eringen (1967), the constitutive and field equations of a micropolar viscoelastic solid in the absence of body forces and body couples, are as under

$$t_{kl} = \lambda u_{r,r}\delta_{kl} + \mu(u_{k,l} + u_{l,k}) + \kappa(u_{l,k} - \epsilon_{klr}\phi_r) \quad \dots (1)$$

$$m_{kl} = \alpha\phi_{r,r}\delta_{kl} + \beta\phi_{k,l} + \gamma\phi_{l,k} \quad \dots (2)$$

$$(c_1^2 + c_3^2)\nabla(\nabla.\mathbf{u}) - (c_2^2 + c_3^2)\nabla\times(\nabla\times\mathbf{u}) + c_3^2\nabla\times\boldsymbol{\phi} = \ddot{\mathbf{u}} \quad \dots (3)$$

$$(c_4^2 + c_5^2)\nabla(\nabla.\boldsymbol{\phi}) - c_4^2\nabla\times(\nabla\times\boldsymbol{\phi}) + \omega_0^2\nabla\times\mathbf{u} - \mathbf{2}\omega_0^2\boldsymbol{\phi} = \ddot{\boldsymbol{\phi}} \quad \dots (4)$$

where

$$c_1^2 = \frac{(\lambda + 2\mu)}{\rho};\ c_2^2 = \frac{\mu}{\rho};\ c_3^2 = \frac{\kappa}{\rho};$$

$$c_4^2 = \frac{\gamma}{\rho j};\ c_5^2 = \frac{(\alpha+\beta)}{\rho j};\ \omega_0^2 = \frac{\kappa}{\rho j};$$

$$\lambda = \lambda^* + \lambda_\upsilon^*\left(\frac{\partial}{\partial t}\right);\ \mu = \mu^* + \mu_\upsilon^*\left(\frac{\partial}{\partial t}\right);$$

$$\kappa = \kappa^* + \kappa_\upsilon^*\left(\frac{\partial}{\partial t}\right);\ \alpha = \alpha^* + \alpha_\upsilon^*\left(\frac{\partial}{\partial t}\right);$$

$$\beta = \beta^* + \beta_\upsilon^*\left(\frac{\partial}{\partial t}\right);\ \gamma = \gamma^* + \gamma_\upsilon^*\left(\frac{\partial}{\partial t}\right);$$

$$\nabla = i\left(\frac{\partial}{\partial x}\right) + k\left(\frac{\partial}{\partial z}\right) \quad \dots (5)$$

$\lambda^*, \mu^*, \kappa^*, \alpha^*, \beta^*, \gamma^*, \lambda_\upsilon^*, \mu_\upsilon^*, \kappa_\upsilon^*, \alpha_\upsilon^*, \beta_\upsilon^*$ and γ_υ^* are material constants, ρ is the density and j the rotational inertia. $\mathbf{u}$ and $\boldsymbol{\phi}$ are displacement and microrotation vectors respectively. Superposed dots on right hand side of equations (3) and (4) represent the second order partial derivative with respect to time.

Taking $\mathbf{u} = (u, 0, w)$ and $\boldsymbol{\phi} = (0, \phi_2, 0)$ and introducing potentials $\phi(x,z,t)$ and $\psi(x,z,t)$ which are related to displacement components as

$$u = \frac{\partial\phi}{\partial x} + \frac{\partial\psi}{\partial z} \text{ and } w = \frac{\partial\phi}{\partial z} - \frac{\partial\psi}{\partial x} \quad \dots (6)$$

With the help of displacement components given by (6) in (3) and (4), we get

$$\left(\nabla^2 - \frac{1}{(c_1^2 + c_3^2)}\frac{\partial^2}{\partial t^2}\right)\phi = 0 \quad \dots (7)$$

$$\left(\nabla^2 - \frac{1}{(c_2^2 + c_3^2)}\frac{\partial^2}{\partial t^2}\right)\psi - p\phi_2 = 0 \quad \dots (8)$$

$$\left(\nabla^2 - 2q - \frac{1}{c_4^2}\frac{\partial^2}{\partial t^2}\right)\phi_2 + q\nabla^2\psi = 0 \quad \dots (9)$$

where

$$p = \frac{\mu}{\mu + \kappa};\ q = \frac{\kappa}{\gamma} \quad \dots (10)$$

Assuming the time variation as

$$\phi(x,z,t) = \bar{\phi}(x,z)\exp(i\omega t)$$
$$\psi(x,z,t) = \bar{\psi}(x,z)\exp(i\omega t)$$
$$\phi_2(x,z,t) = \bar{\phi}_2(x,z)\exp(i\omega t) \quad \dots (11)$$

Using (11) in (7) to (9), we obtain

$$\left(\nabla^2 + \left(\omega^2/V_1^2\right)\right)\bar{\phi} = 0 \quad \dots (12)$$

$$(\nabla^4 + \omega^2 B\nabla^2 + \omega^4 C)(\bar{\psi}, \bar{\phi}_2) = 0 \quad \dots (13)$$

where

$$B = \frac{q(p-2)}{\omega^2} + \frac{1}{(c_2^2 + c_3^2)} + \frac{1}{c_4^2}$$

$$C = \frac{1}{(c_2^2 + c_3^2)}\left(\frac{1}{c_4^2} - \frac{2q}{\omega^2}\right) \quad \dots (14)$$

and $V_1^2 = c_1^2 + c_3^2$ ... (15)

In an unbounded medium, the solution of (12) corresponds to modified longitudinal displacement wave (LD wave) propagating with velocity V_1.

Writing the solution of (13) as

$$\bar{\psi} = \bar{\psi}_1 + \bar{\psi}_2 \quad \dots (16)$$

where

$\bar{\psi}_1$ and $\bar{\psi}_2$ satisfy

$$(\nabla^2 + \delta_1^2)\bar{\psi}_1 = 0 \quad \dots (17)$$

$$(\nabla^2 + \delta_2^2)\bar{\psi}_2 = 0 \quad \dots (18)$$

and

$$\delta_1^2 = \lambda_1^2\omega^2;\ \delta_2^2 = \lambda_2^2\omega^2 \quad \dots (19)$$

$$\lambda_1^2 = \frac{1}{2}\left[B + \sqrt{B^2 - 4C}\right];$$

$$\lambda_2^2 = \frac{1}{2}\left[B - \sqrt{B^2 - 4C}\right] \quad \dots (20)$$

From (8) we obtain

$$\bar{\phi}_2 = E\bar{\psi}_1 + F\bar{\psi}_2$$

$$\text{where } E = \frac{\left(\frac{\omega^2}{c_2^2 + c_3^2} - \delta_1^2\right)}{p};\ F = \frac{\left(\frac{\omega^2}{c_2^2 + c_3^2} - \delta_2^2\right)}{p} \quad \dots (21)$$

Thus there are two waves propagating with velocities λ_1^{-1} and λ_2^{-1}, each consisting of transverse displacement ψ and transverse microrotation ϕ_2. Following Parfitt and Eringen(1969), these waves are modified coupled transverse displacement wave and transverse microrotational waves (CD I and CD II waves) respectively.

For medium M_1 (Fluid saturated incompressible porous medium): Following de Boer and Ehlers (1990b), the governing equations in a fluid-saturated incompressible porous medium are

$$\mathrm{div}(\eta^S \dot{\mathbf{x}}_S + \eta^F \dot{\mathbf{x}}_F) = 0 \quad \text{... (22)}$$

$$\mathrm{div}\mathbf{T}_E^S - \eta^S \,\mathrm{grad}\, p + \rho^S(\mathbf{b} - \ddot{\mathbf{x}}_s) - \mathbf{P}_E^F = 0, \quad \text{... (23)}$$

$$\mathrm{div}\mathbf{T}_E^F - \eta^F \,\mathrm{grad}\, p + \rho^F(\mathbf{b} - \ddot{\mathbf{x}}_F) + \mathbf{P}_E^F = 0, \quad \text{... (24)}$$

where $\dot{\mathbf{x}}_i$ and $\ddot{\mathbf{x}}_i$ $(i = S, F)$ denote the velocities and accelerations, respectively of solid (S) and fluid (F) phases of the porous aggregate and p is the effective pore pressure of the incompressible pore fluid. ρ^S and ρ^F are the densities of the solid and fluid phases respectively and $\mathbf{b}$ is the body force per unit volume. $\mathbf{T}_E^S$ and $\mathbf{T}_E^F$ are the effective stress in the solid and fluid phases respectively, $\mathbf{P}_E^F$ is the effective quantity of momentum supply and η^S and η^F are the volume fractions satisfying

$$\eta^S + \eta^F = 1 \quad \text{... (27)}$$

If $\mathbf{u}_S$ and $\mathbf{u}_F$ are the displacement vectors for solid and fluid phases, then

$$\dot{x}_S = \dot{\mathbf{u}}_S, \ddot{\mathbf{x}}_s = \ddot{\mathbf{u}}_s, \dot{\mathbf{x}}_F = \dot{\mathbf{u}}_F, \ddot{\mathbf{x}}_F = \ddot{\mathbf{u}}_F \quad \text{... (28)}$$

The constitutive equations for linear isotropic, elastic incompressible porous medium are given by de Boer, Ehlers and Liu (1993) as

$$\mathbf{T}_E^S = 2\mu^S \mathbf{E}_S + \lambda^S(E_S.\mathbf{I})\mathbf{I}, \quad \text{... (29)}$$

$$\mathbf{T}_E^F = 0, \quad \text{... (30)}$$

$$\mathbf{P}_E^F = -\mathbf{S}_v(\dot{\mathbf{u}}_F - \dot{\mathbf{u}}_S), \quad \text{... (31)}$$

where λ^S and μ^S are the macroscopic Lame's parameters of the porous solid and $\mathbf{E}_S$ is the linearized Langrangian strain tensor defined as

$$\mathbf{E}_S = \frac{1}{2}(\mathrm{grad}\, \mathbf{u}_S + \mathrm{grad}^T \mathbf{u}_S), \quad \text{... (32)}$$

In the case of isotropic permeability, the tensor $\mathbf{S}_v$ describing the coupled interaction between the solid and fluid is given by de Boer and Ehlers (1990b) as

$$\mathbf{S}_v = \frac{(\eta^F)^2 \gamma^{FR}}{K^F}\mathbf{I}, \quad \text{... (33)}$$

where γ^{FR} is the specific weight of the fluid and K^F is the Darcy's permeability coefficient of the porous medium.

Making the use of (28) in equations (22)-(24), and with the help of (29)-(32), we obtain

$$\mathrm{div}(\eta^S \dot{\mathbf{u}}_S + \eta^F \dot{\mathbf{u}}_F) = 0, \quad \text{... (34)}$$

$$(\lambda^S + \mu^S)\mathrm{grad\, div}\, \mathbf{u}_S + \mu^S \mathrm{div\, grad}\, \mathbf{u}_S - \eta^S \mathrm{grad}\, p + \rho^S(\mathbf{b} - \ddot{\mathbf{u}}_s) + S_v(\dot{\mathbf{u}}_F - \dot{\mathbf{u}}_S) = 0, \quad (35)$$

$$-\eta^F \mathrm{grad}\, p + \rho^F(\mathbf{b} - \ddot{\mathbf{u}}_F) - S_v(\dot{\mathbf{u}}_F - \dot{\mathbf{u}}_S) = 0 \quad \text{... (36)}$$

For the two dimensional problem, we assume the displacement vector $\mathbf{u}_i$ $(i = F, S)$ as

$$\mathbf{u}_i = (u^i, 0, w^i) \text{ where } i = F, S. \quad \text{... (37)}$$

Equations (34) - (36) with the help of equation (37) in the absence of body forces take the form

$$\eta^S\left[\frac{\partial^2 u^S}{\partial x \partial t} + \frac{\partial^2 w^S}{\partial z \partial t}\right] + \eta^F\left[\frac{\partial^2 u^F}{\partial x \partial t} + \frac{\partial^2 w^F}{\partial z \partial t}\right] = 0, \quad \text{... (38)}$$

$$\eta^F \frac{\partial p}{\partial x} + \rho^F \frac{\partial^2 u^F}{\partial t^2} + S_v\left[\frac{\partial u^F}{\partial t} - \frac{\partial u^S}{\partial t}\right] = 0, \quad \text{... (39)}$$

$$\eta^F \frac{\partial p}{\partial z} + \rho^F \frac{\partial^2 w^F}{\partial t^2} + S_v\left[\frac{\partial w^F}{\partial t} - \frac{\partial w^S}{\partial t}\right] = 0, \quad \text{... (40)}$$

$$(\lambda^S + \mu^S)\frac{\partial \theta^S}{\partial x} + \mu^S \nabla^2 u^S - \eta^S \frac{\partial p}{\partial x} - \rho^S \frac{\partial^2 u^S}{\partial t^2} + S_v\left[\frac{\partial u^F}{\partial t} - \frac{\partial u^S}{\partial t}\right] = 0, \quad \text{... (41)}$$

$$(\lambda^S + \mu^S)\frac{\partial \theta^S}{\partial z} + \mu^S \nabla^2 w^S - \eta^S \frac{\partial p}{\partial z} - \rho^S \frac{\partial^2 w^S}{\partial t^2} + S_v\left[\frac{\partial w^F}{\partial t} - \frac{\partial w^S}{\partial t}\right] = 0, \quad \text{... (42)}$$

where

$$\theta^S = \frac{\partial(u^S)}{\partial x} + \frac{\partial(w^S)}{\partial z} \quad \text{... (43)}$$

and

$$\nabla^2 = \frac{\partial^2}{\partial x^2} + \frac{\partial^2}{\partial z^2} \quad \text{... (44)}$$

Also, ${t_{zz}}^S$ and ${t_{zx}}^S$ the normal and tangential stresses in the solid phase are as under

$${t_{zz}}^S = \lambda^S\left(\frac{\partial u^S}{\partial x} + \frac{\partial w^S}{\partial z}\right) + 2\mu^S \frac{\partial w^S}{\partial z} \quad \text{... (45)}$$

$${t_{zx}}^S = \mu^S\left(\frac{\partial u^S}{\partial z} + \frac{\partial w^S}{\partial x}\right) \quad \text{... (46)}$$

The displacement components u^j and w^j are related to the dimensional potential ϕ^j and ψ^j as

$$u^j = \frac{\partial \phi^j}{\partial x} + \frac{\partial \psi^j}{\partial z} \text{ and } w^j = \frac{\partial \phi^j}{\partial z} - \frac{\partial \psi^j}{\partial x} \quad j = S, F \quad \text{... (47)}$$

Using eq. (47) in equations (38)-(42), we obtain the following equations determining $\phi^S, \phi^F, \psi^S, \psi^F$ and p as:

$$\nabla^2 \phi^S - \frac{1}{{C_1}^2}\frac{\partial^2 \phi^S}{\partial t^2} - \frac{S_v}{(\lambda^S + 2\mu^S)(\eta^F)^2}\frac{\partial \phi^S}{\partial t} = 0 \quad \text{... (48)}$$

$$\phi^F = -\frac{\eta^S}{\eta^F}\phi^S \quad \text{... (49)}$$

$$\mu^S \nabla^2 \psi^S - \rho^S \frac{\partial^2 \psi^S}{\partial t^2} + S_v\left[\frac{\partial \psi^F}{\partial t} - \frac{\partial \psi^S}{\partial t}\right] = 0 \quad \text{... (50)}$$

$$\rho^F \frac{\partial^2 \psi^F}{\partial t^2} + S_v\left[\frac{\partial \psi^F}{\partial t} - \frac{\partial \psi^S}{\partial t}\right] = 0 \quad \text{... (51)}$$

$$(\eta^F)^2 p - \eta^S \rho^F \frac{\partial^2 \phi^S}{\partial t^2} - S_v \frac{\partial \phi^S}{\partial t} = 0 \quad \text{... (52)}$$

where

$$C_1 = \sqrt{\frac{(\eta^F)^2(\lambda^S + 2\mu^S)}{(\eta^F)^2\rho^S + (\eta^S)^2\rho^F}} \quad \text{... (53)}$$

Assuming the solution of the system of equations (48) - (52) in the form

$$\left(\phi^S, \phi^F, \psi^S, \psi^F, p\right) = \left({\phi_1}^S, {\phi_1}^F, {\psi_1}^S, {\psi_1}^F, p_1\right)\exp(i\omega t) \quad \text{... (54)}$$

where ω is the complex circular frequency.

Making the use of (54) in equations (48)-(52), we obtain

$$\left[\nabla^2 + \frac{\omega^2}{{C_1}^2} - \frac{i\omega S_v}{(\lambda^S + 2\mu^S)(\eta^F)^2}\right]{\phi_1}^S = 0 \quad \text{... (55)}$$

$$[\mu^S\nabla^2 + \rho^S\omega^2 - i\omega S_v]{\psi_1}^S = -i\omega S_v {\psi_1}^F \quad \text{... (56)}$$

$$[-\omega^2\rho^F + i\omega S_v]{\psi_1}^F - i\omega S_v {\psi_1}^S = 0 \quad \text{... (57)}$$

$$(\eta^F)^2 p_1 + \eta^S\rho^F\omega^2{\phi_1}^S - i\omega S_v {\phi_1}^S = 0 \quad \text{... (58)}$$

$${\phi_1}^F = -\frac{\eta^S}{\eta^F}{\phi_1}^S \quad \text{... (59)}$$

Equation (55) corresponds to longitudinal wave propagating with velocity $\overline{V}_1$, given by

$${\overline{V}_1}^2 = \frac{1}{G_1} \quad \text{... (60)}$$

where $G_1 = \left[\frac{1}{{C_1}^2} - \frac{iS_v}{\omega(\lambda^S+2\mu^S)(\eta^F)^2}\right]$ ... (61)

From equation (56) and (57), we obtain

$$\left[\nabla^2 + \frac{\omega^2}{{\overline{V}_2}^2}\right]{\psi_1}^S = 0, \quad \text{... (62)}$$

Equation (62) corresponds to transverse wave propagating with velocity $\overline{V}_2$, given by ${\overline{V}_2}^2 = 1/G_2$

where

$$G_2 = \left\{\frac{\rho^S}{\mu^S} - \frac{iS_v}{\mu^S\omega} - \frac{{S_v}^2}{\mu^S(-\rho^S\omega^2 + i\omega S_v)}\right\} \quad \text{... (63)}$$

FORMULATION OF THE PROBLEM

Consider a two dimensional problem by taking the z-axis pointing into the lower half-space and the plane interface z=0 separating the uniform micropolar viscoelastic solid half space medium M_2 (z<0) and fluid saturated porous half space medium M_1 (z>0). Consider a longitudinal wave or transverse wave propagating through the medium M_1, incident at the plane z=0 and making an angle θ_0 with normal to the surface. Corresponding to incident longitudinal wave or transverse wave, we get two reflected waves in the medium M_1 and three transmitted waves in medium M_2 as shown in fig.1.

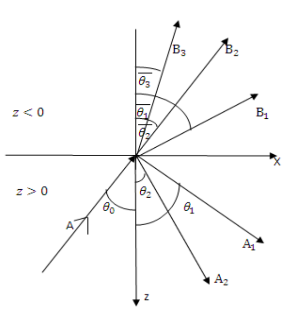

Figure 1: Geometry of the problem

In medium M_2

$$\phi = B_1\exp\{i\delta_1(x\sin\bar{\theta}_1 - z\cos\bar{\theta}_1) + i\bar{\omega}_1 t\}, \quad \text{... (64)}$$

$$\psi = B_2\exp\{i\delta_2(x\sin\bar{\theta}_2 - z\cos\bar{\theta}_2) + i\bar{\omega}_2 t\} + B_3\exp\{i\delta_3(x\sin\bar{\theta}_3 - z\cos\bar{\theta}_3) + i\bar{\omega}_3 t\}, \quad \text{... (65)}$$

$$\Phi_2 = EB_2\exp\{i\delta_2(x\sin\bar{\theta}_2 - z\cos\bar{\theta}_2) + i\bar{\omega}_2 t\} + FB_3\exp\{i\delta_3(x\sin\bar{\theta}_3 - z\cos\bar{\theta}_3) + i\bar{\omega}_3 t\}, \quad \text{... (66)}$$

In medium M_1

$$\{\phi^S, \phi^F, p\} = \{1, m_1, m_2\}[A_{01}\exp\{ik_1(x\sin\theta_0 - z\cos\theta_0) + i\omega_1 t\} + A_1\exp\{ik_1(x\sin\theta_1 + z\cos\theta_1) + i\omega_1 t\}], \quad \text{... (67)}$$

$$\{\psi^S, \psi^F\} = \{1, m_3\}[B_{01}\exp\{ik_2(x\sin\theta_0 - z\cos\theta_0) + i\omega_2 t\} + A_2\exp\{ik_2(x\sin\theta_2 + z\cos\theta_2) + i\omega_2 t\}], \quad \text{... (68)}$$

where

$$m_1 = -\frac{\eta^S}{\eta^F}; \; m_2 = -\left[\frac{\eta^S{\omega_1}^2\rho^F - i\omega_1 S_v}{(\eta^F)^2}\right]; \; m_3 = \frac{i\omega_2 S_v}{i\omega_2 S_v - {\omega_2}^2\rho^F}; \quad \text{... (69)}$$

and B_1, B_2, B_3 are amplitudes of transmitted P-wave, transmitted coupled transverse and micro-rotation waves respectively. Also A_{01} or B_{01}, A_1 and A_2 are amplitudes of incident P-wave or SV-wave, reflected P-wave and reflected SV-wave respectively and to be determined from boundary conditions.

BOUNDARY CONDITIONS

Boundary conditions appropriate here are the continuity of displacement, micro rotation and stresses at the interface separating medium M_1 and M_2. These boundary conditions at z=0 can be written in mathematical form as

$$t_{zz} = {t_{zz}}^S - p; \; t_{zx} = {t_{zx}}^S, \; m_{zy} = 0$$

$${t_{zz}}^S - p = K_n(w - w^S); \; {t_{zx}}^S = K_t(u - u^S) \quad \text{... (70)}$$

In order to satisfy the boundary conditions, the extension of the Snell's law will be

$$\frac{\sin\theta_0}{v_0} = \frac{\sin\theta_1}{v_1} = \frac{\sin\theta_2}{v_2} = \frac{\sin\bar{\theta}_1}{\bar{v}_1} = \frac{\sin\bar{\theta}_2}{\bar{v}_2} = \frac{\sin\bar{\theta}_3}{\bar{v}_3} \quad \text{... (71)}$$

where $\bar{v}_2 = \frac{1}{\lambda_2}$; $\bar{v}_3 = \frac{1}{\lambda_3}$

For longitudinal wave,

$$v_0 = v_1; \; \theta_0 = \theta_1 \quad \text{... (72)}$$

For transverse wave,

$$v_0 = v_2; \; \theta_0 = \theta_2 \quad \text{... (73)}$$

Also

$$\delta_1\bar{v}_1 = \delta_2\lambda_2^{-1} = \delta_3\lambda_3^{-1} = k_1 v_1 = k_2 v_2 = \omega, \text{ at } z = 0 \quad \text{... (74)}$$

Making the use of potentials given by equations (64)-(68) in equations (1)-(2) and (6) and (45)-(47) and (67) and then using the boundary conditions given by equation (70) and using (71)-(74), we get a system of five non homogeneous which can be written as

$$\sum_{j=0}^{5} a_{ij} Z_j = Y_i, (i = 1,2,3,4,5) \quad \ldots (75)$$

where

$$Z_1 = \frac{B_1}{B_0};\ Z_2 = \frac{B_2}{B_0};\ Z_3 = \frac{B_3}{B_0};\ Z_4 = \frac{A_1}{B_0};$$
$$Z_5 = \frac{A_2}{B_0} \quad \ldots (76)$$

where $B_0 = A_{01}$ or B_{01} is amplitude of incident P-wave or SV-wave respectively.

i.e. Z_1 to Z_5 be the amplitude ratios of reflected modified longitudinal displacement wave, reflected CD I wave at an angle θ_2, reflected CD II wave at an angle θ_3, refracted P-wave and refracted SV-wave, respectively and a_{ij} in non-dimensional form are as

$$a_{11} = \frac{-\lambda\delta_1^{\,2} - (2\mu+\kappa)\left(\delta_1^{\,2}\cos^2\bar{\theta}_1\right)}{\mu\delta_1^{\,2}};$$
$$a_{12} = \frac{(2\mu+\kappa)\delta_2^{\,2}\sin\bar{\theta}_2\cos\bar{\theta}_2}{\mu\delta_1^{\,2}}$$
$$a_{13} = \frac{(2\mu+\kappa)\delta_3^{\,2}\sin\bar{\theta}_3\cos\bar{\theta}_3}{\mu\delta_1^{\,2}};$$
$$a_{14} = \frac{k_1^2\left(\lambda^S + 2\mu^S\cos^2\theta_1\right) + m_2}{\mu\delta_1^{\,2}}$$
$$a_{15} = \frac{-2\mu^S k_2^2\sin\theta_2\cos\theta_2}{\mu\delta_1^{\,2}};$$
$$a_{21} = \frac{(2\mu+\kappa)\delta_1^{\,2}\sin\bar{\theta}_1\cos\bar{\theta}_1}{\mu\delta_1^{\,2}}$$
$$a_{22} = \frac{\mu\delta_2^{\,2}\cos 2\bar{\theta}_2 + \kappa\delta_2^{\,2}\cos^2\bar{\theta}_2 - \kappa E}{\mu\delta_1^{\,2}};$$
$$a_{23} = \frac{\mu\delta_3^{\,2}\cos 2\bar{\theta}_3 + \kappa\delta_3^{\,2}\cos^2\bar{\theta}_3 - \kappa F}{\mu\delta_1^{\,2}}$$
$$a_{24} = \frac{\mu^S k_1^2\sin 2\theta_1}{\mu\delta_1^{\,2}};\ a_{25} = \frac{\mu^S k_2^2\cos 2\theta_2}{\mu\delta_1^{\,2}}$$
$$a_{31} = 0;\ a_{32} = \cos\bar{\theta}_2;\ a_{33} = \frac{\delta_3 F\cos\bar{\theta}_3}{\delta_2 E};$$
$$a_{34} = 0;\ a_{35} = 0$$
$$a_{41} = \frac{\lambda\delta_1^{\,2} + (2\mu+\kappa)\left(\delta_1^{\,2}\cos^2\bar{\theta}_1\right) + k_n i\,\delta_1\cos\bar{\theta}_1}{k_n\,\delta_1};$$
$$a_{42} = \frac{-(2\mu+\kappa)\delta_2^{\,2}\sin\bar{\theta}_2\cos\bar{\theta}_2 - k_n i\,\delta_2\sin\bar{\theta}_2}{k_n\,\delta_1};$$
$$a_{43} = \frac{-(2\mu+\kappa)\delta_3^{\,2}\sin\bar{\theta}_3\cos\bar{\theta}_3 - k_n i\,\delta_3\sin\bar{\theta}_3}{k_n\,\delta_1};$$
$$a_{44} = \frac{i\,k_1\cos\theta_1}{\delta_1};\ a_{45} = -\frac{i\,k_2\sin\theta_2}{\delta_1};$$
$$a_{51} = \frac{-(2\mu+\kappa)\delta_1^{\,2}\sin\bar{\theta}_1\cos\bar{\theta}_1 - ik_t\,\delta_1\sin\bar{\theta}_1}{k_t\,\delta_1};$$
$$a_{52} = \frac{-\mu\delta_2^{\,2}\cos 2\bar{\theta}_2 - \kappa\delta_2^{\,2}\cos^2\bar{\theta}_2 + \kappa E - k_t i\,\delta_2\cos\bar{\theta}_2}{k_t\,\delta_1};$$
$$a_{53} = \frac{-\mu\delta_3^{\,2}\cos 2\bar{\theta}_3 - \kappa\delta_3^{\,2}\cos^2\bar{\theta}_3 + \kappa F - k_t i\,\delta_3\cos\bar{\theta}_3}{k_t\,\delta_1};$$
$$a_{54} = \frac{i\,k_1\sin\theta_1}{\delta_1};\ a_{55} = \frac{i\,k_2\cos\theta_2}{\delta_1};$$

For incident P wave

$Y_1 = -a_{14}$; $Y_2 = a_{24}$; $Y_3 = a_{34}$; $Y_4 = a_{44}$; $Y_5 = -a_{54}$

For incident SV wave

$Y_1 = a_{15}$; $Y_2 = -a_{25}$; $Y_3 = a_{35}$; $Y_4 = -a_{45}$; $Y_5 = a_{55}$ ... (77)

PARTICULAR CASES

Case I: Normal force stiffness $(K_n \neq 0, K_t \to \infty)$

In this case, we get a system of five non homogeneous equations as in given by equation (77) with some a_{ij} changed as

$$a_{51} = -i\sin\bar{\theta}_1;\ a_{52} = \frac{-i\,\delta_2\cos\bar{\theta}_2}{\delta_1};$$
$$a_{53} = \frac{-i\,\delta_3\cos\bar{\theta}_3}{\delta_1}; \quad \ldots (78)$$

Case II: Transverse force stiffness $(K_t \neq 0, K_n \to \infty)$

In this case, a system of five non homogeneous equations as those given by equation (77) is obtained but some a_{ij} changed as

$$a_{41} = \frac{i\,\delta_1\cos\bar{\theta}_1}{\delta_1};\ a_{42} = \frac{-i\,\delta_2\sin\bar{\theta}_2}{\delta_1};$$
$$a_{43} = \frac{-i\,\delta_3\sin\bar{\theta}_3}{\delta_1} \quad \ldots (79)$$

Case III: Welded contact $(K_n \to \infty, K_t \to \infty)$

Again in this case, a system of five non homogeneous equations is obtained as in equation (67) with some a_{ij} changed as

$$a_{41} = \frac{i\,\delta_1\cos\bar{\theta}_1}{\delta_1};\ a_{42} = \frac{-i\,\delta_2\sin\bar{\theta}_2}{\delta_1};$$
$$a_{43} = \frac{-i\,\delta_3\sin\bar{\theta}_3}{\delta_1};$$
$$a_{51} = -i\sin\bar{\theta}_1;\ a_{52} = \frac{-i\,\delta_2\cos\bar{\theta}_2}{\delta_1};$$

$$a_{53} = \frac{-i\,\delta_3 \cos\bar{\theta}_3}{\delta_1}\ ; \qquad \dots (80)$$

Special case:-

CASE-1

If pores are absent or gas is filled in the pores then ρ^F is very small as compared to ρ^S and can be neglected, so the relation (41) gives us

$$C = \sqrt{\frac{\lambda^S + 2\mu^S}{\rho^S}}. \qquad \dots (81)$$

In this situation the problem reduces to the problem of empty porous solid half space lying over micropolar elastic solid half space.

CASE-2

When upper half space is micropolar elastic solid. In this case boundary conditions remain same and hence a_{ij} in equation (77) are same.

NUMERICAL RESULTS AND DISCUSSION

The theoretical results obtained above indicate that the amplitude ratios $Z_i\ (i = 1,2,3,4,5\ )$ depend on the angle of incidence of incident wave and material properties of half spaces. In order to study in more detail the behaviour of various amplitude ratios, we have computed them numerically for a particular model for which the values of various physical parameters are as under In medium M_2, the physical parameters for micropolar viscoelastic elastic solid are taken from Gauthier (1982) as

$$\lambda^* = 7.59 \times 10^{11}\,\frac{\text{dyne}}{\text{cm}^2},$$
$$\mu^* = 1.89 \times 10^{11}\ \text{dyne/cm}^2,$$
$$\kappa^* = 0.0149 \times 10^{11}\text{dyne/cm}^2, \rho = 2.19\text{gm/cm}^3$$
$$\gamma^* = 0.0268 \times 10^{11}\text{dyne}, j = 0.0196\text{cm}^2.$$
$$\lambda = \lambda^*\left(1 + \frac{i}{Q_1}\right), \mu = \mu^*\left(1 + \frac{i}{Q_2}\right),$$
$$\kappa = \kappa^*\left(1 + \frac{i}{Q_3}\right), \gamma = \gamma^*\left(1 + \frac{i}{Q_4}\right), \qquad \dots (79)$$

where the quality factors $Q_i(i = 1,2,3,4)$ are taken arbitrarily as

$Q_1 = 5, Q_2 = 10, Q_3 = 15, Q_4 = 13.$

In mediumM_1, the physical constants for fluid saturated incompressible porous medium are taken from de Boer, Ehlers and Liu (1993) as

$$\eta^s = 0.67, \eta^F = 0.33, \qquad \rho^s = 1.34\,\frac{\text{Mg}}{\text{m}^3},$$
$$\rho^F = 0.33\ \text{Mg/m}^3, \lambda^s = 5.5833\ \text{MN/m}^2,$$
$$K^F = \frac{0.01\text{m}}{\text{s}}, \qquad \gamma^{FR} = \frac{10.00\text{KN}}{\text{m}^3}$$
$$\mu^s = \frac{8.3750\text{N}}{\text{m}^2} \qquad \dots (80)$$

A computer programme in MATLAB has been developed to calculate the modulus of amplitude ratios of various reflected and transmitted waves for the particular model and to depict graphically. In figures (2)-(22), dashed dotted line shows the general case (Gen) when medium-I is fluid saturated porous solid and medium-II is micropolar viscoelastic solid half space. In these figures dotted line shows the case when medium-I becomes empty porous solid and medium-II remains same. In these figures P wave (longitudinal wave) is incident wave. Figure (2)-(5) shows the variation of $|Z_1|$ with respect to angle of incidence which varies from $\theta = 0^0$ to $\theta = 90^0$. These figures show the effect of porosity which is very clear. Also after comparing the figures (2)-(5), the effect of stiffness is clear. In figure (2), the contact between two half space is imperfect. Figure (3) shows the variation of $|Z_1|$ when contact between half spaces is Normal Force Stiffness (NFS). Figure (4) corresponding to Transverse Force Stiffness (TFS) contact. Figure (5) shows the variation of $|Z_1|$ when the contact between two half spaces is Welded (Welded). In figures (2)-(5) effect of fluid filled in pores (porosity) as well as effect of stiffness is very clear. Figure (6)-(9) shows the variation of $|Z_2|$ with respect to angle of incident P wave. In these figures also, the effect of porosity and effect of stiffness is clear. In all cases of stiffness (imperfect boundary, normal force stiffness, transfers force stiffness, welded contact) the value of $|Z_2|$ are different. Figure (10) to (13) shows the variation of $|Z_3|$ with respect to angle of incidence of P wave. In all these figures, the effect of porosity and stiffness is very clear. The values of $|Z_3|$ are small in case of imperfect interface than all other cases. Figure (14) to (18) shows the variation of $|Z_4|$ i.e. modulus of amplitude ratio for reflected P wave with respect to angle of incident from $\theta = 0^0$ to $\theta = 90^0$. These figures also show the effect of porosity as well as effect of stiffness. Figures (19) to (22) depict the variation of $|Z_5|$ with respect to angle of incident of P wave. In these figures the effect of stiffness and porosity is very clear. In figures (23) to (42), there is a SV wave (transverse wave) incident. In these figure dashed dotted line shows the variation of $|Z_i|$ $(i = 1,2,3,4,5)$ when medium-I is fluid saturated porous solid whereas dotted line shows the case when medium-I becomes empty porous solid (EPS). In all these figures (23) to (42) medium-II to remains same. Also in these figures, imperfect shows the case when interface between two half spaces is imperfect. NFS shows the case when contact between the two half spaces is Normal force stiffness. TFS shows the case when boundary between two half spaces is transverse force stiffness. Welded shows the case of welded contact between the spaces. Figures (23)-(26), (27)-(30), (31)-(34), (35)-(38) and (39)-(42) shows the variation of $|Z_i|$ $(i = 1,2,3,4,5)$ respectively for different cases of stiffness. This figure shows the effect of porosity i.e. fluid filled in the pores of fluid saturated porous solid and effect of stiffness. In figures (43) to (81) dashed dotted lines shows the case when medium-I is fluid situated porous solid and medium-II is micropolar viscoelastic solid. Dotted lines show the case when medium-I remain same but medium-II becomes micropolar elastic solid. These figures show the effect of viscosity of micropolar viscoelastic solid. In figures (43) to (62), P wave is incident and the figure (63) to (81), there is SV wave incident. Figures (43)-(46), (47)-(50), (51)-(54), (55)-(58) and (59)-(62) shows the variation of $|Z_i|$ (i = 1,2,3,4,5) respectively with angle of incidence P wave in four cases of stiffness i.e. imperfect interface, NFS (normal force stiffness), TFS (transverse force stiffness), Welded (welded). In figures (43) to (54), the effect of viscosity and stiffness is evident i.e. for modulus of amplitude ratio corresponding to transmitted wave. But figures (55) to (58) i.e. for corresponding to reflected P wave, the effect of viscosity is negligible. In figures (59) to (62), the effect of viscosity for reflected transverse wave (SV wave) is negligible for imperfect and welded case. But effect of viscosity in NFS, TFS is clear. Figures (63)-(66), (67)-(70), (71)-(74), (75)-(78) and (79)-(81), shows the variation of $|Z_1|, |Z_2|, |Z_3|, |Z_4|$ and $|Z_5|$ respectively in four cases of stiffness. In all these figures i.e. (63 to (81), the effect of stiffness as well as effect of viscosity is clear. Also the effect of viscosity is more for transmitted wave than for reflected waves.

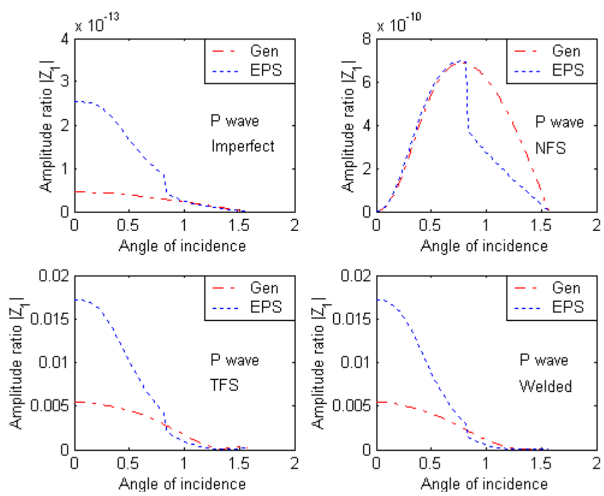

Figure (2)-(5): Variation of the $|Z_1|$ with angle of incidence of the incident longitudinal wave

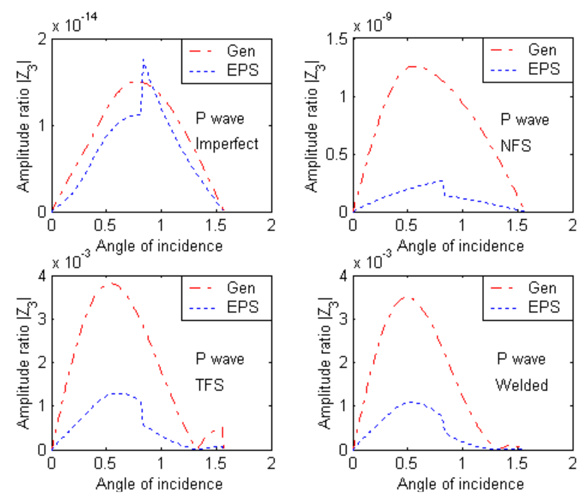

Figure (10)-(13): Variation of the $|Z_3|$ with angle of incidence of the incident longitudinal wave

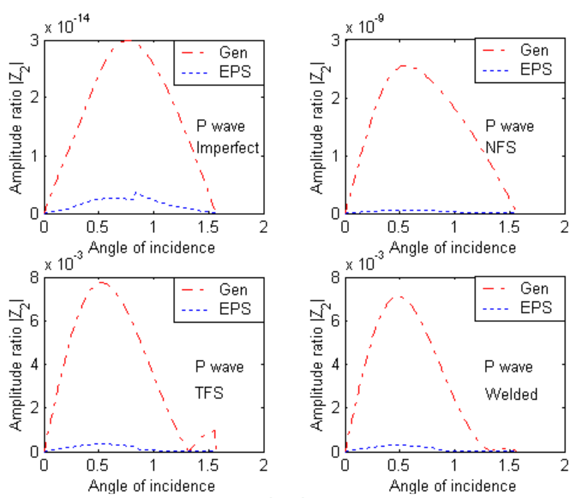

Figure (6)-(9): Variation of the $|Z_2|$ with angle of incidence of the incident longitudinal wave

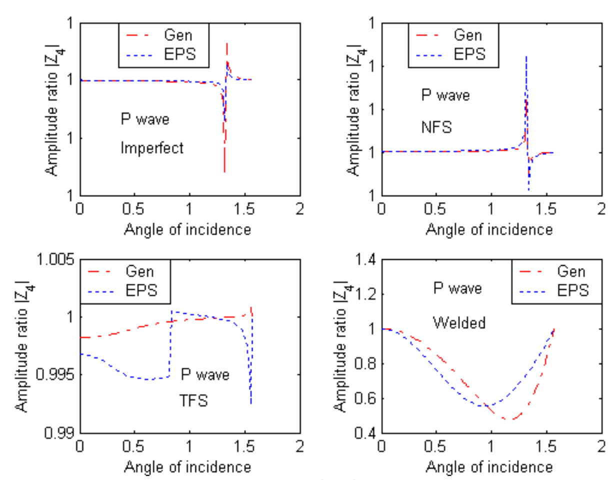

Figure (14)-(18): Variation of the $|Z_4|$ with angle of incidence of the incident longitudinal wave

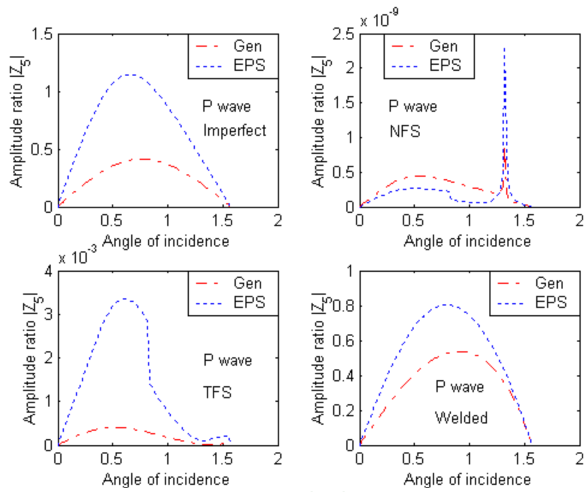

Figure (19)-(22): Variation of the $|Z_5|$ with angle of incidence of the incident longitudinal wave

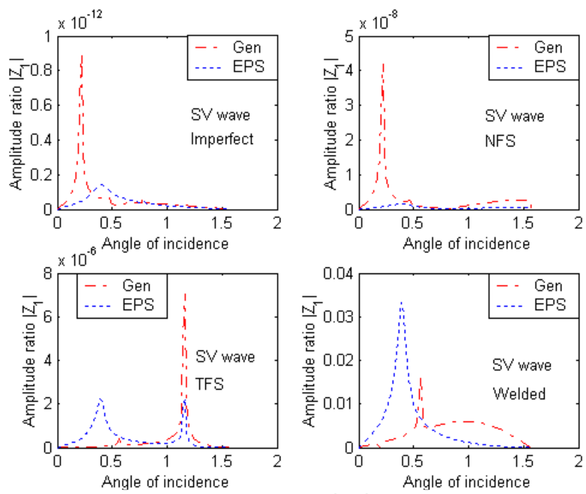

Figure (23)-(26): Variation of the $|Z_1|$ with angle of incidence of the incident transverse wave

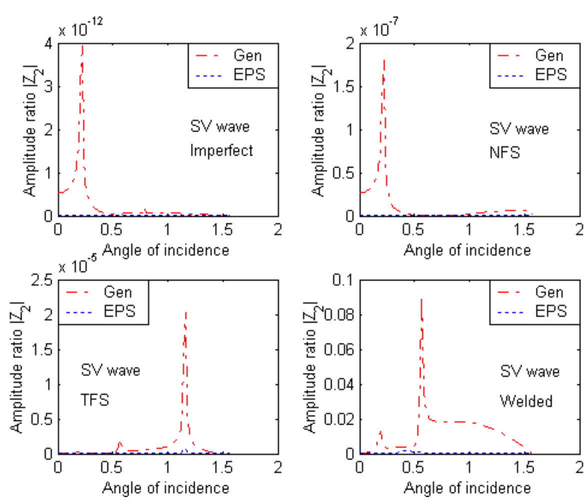

Figure (27)-(30): Variation of the $|Z_2|$ with angle of incidence of the incident transverse wave

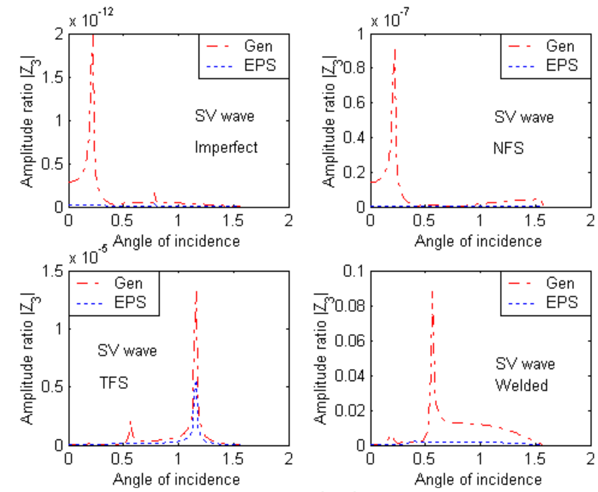

Figure (31)-(34): Variation of the $|Z_3|$ with angle of incidence of the incident transverse wave

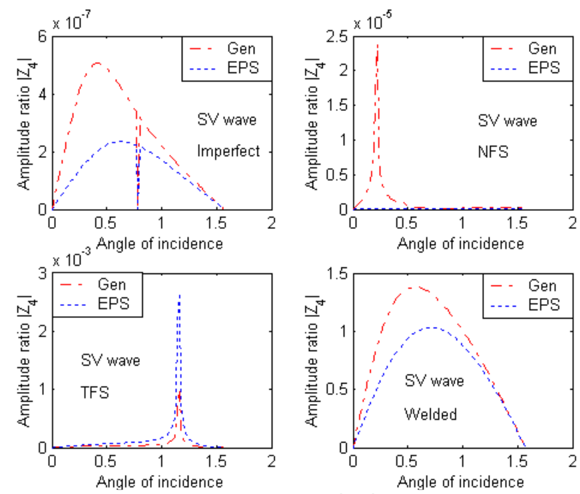

Figure (35)-(38): Variation of the $|Z_4|$ with angle of incidence of the incident transverse wave

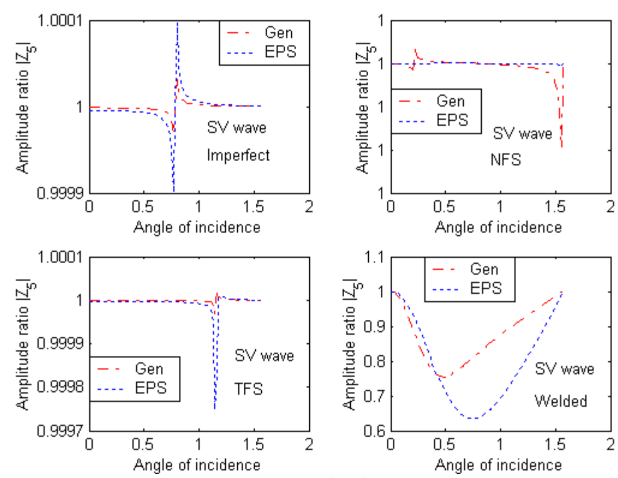

Figure (39)-(42): Variation of the $|Z_5|$ with angle of incidence of the incident transverse wave

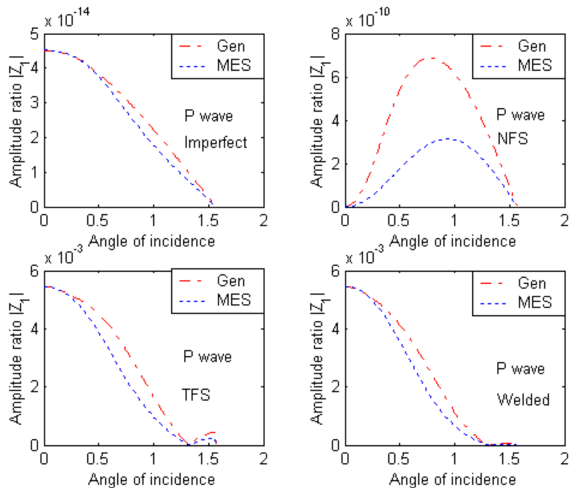

Figure (43)-(46): Variation of the $|Z_1|$ with angle of incidence of the incident longitudinal wave

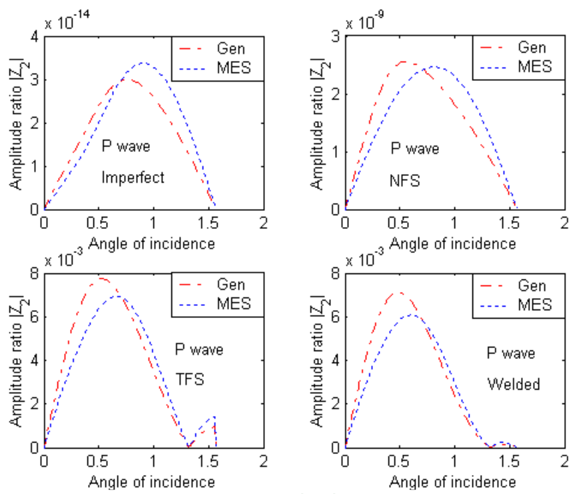

Figure (47)-(50): Variation of the $|Z_2|$ with angle of incidence of the incident longitudinal wave

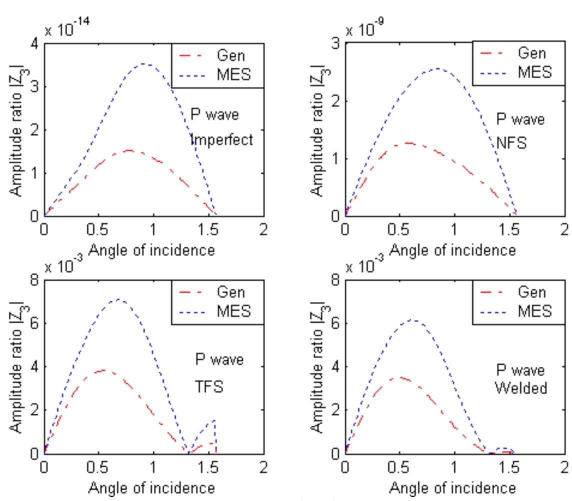

Figure (51)-(54): Variation of the $|Z_3|$ with angle of incidence of the incident longitudinal wave

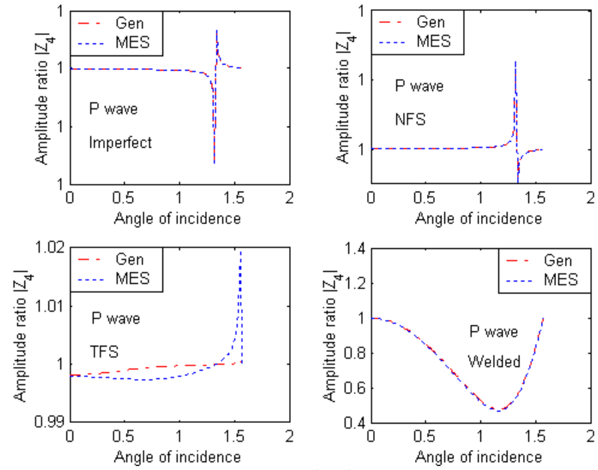

Figure (55)-(58): Variation of the $|Z_4|$ with angle of incidence of the incident longitudinal wave

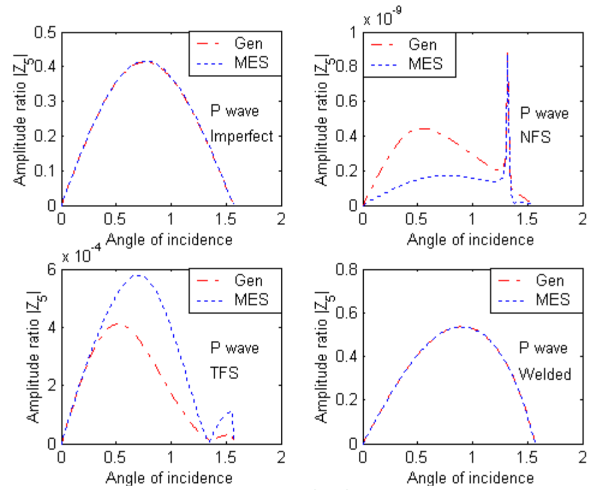

Figure (59)-(62): Variation of the $|Z_5|$ with angle of incidence of the incident longitudinal wave

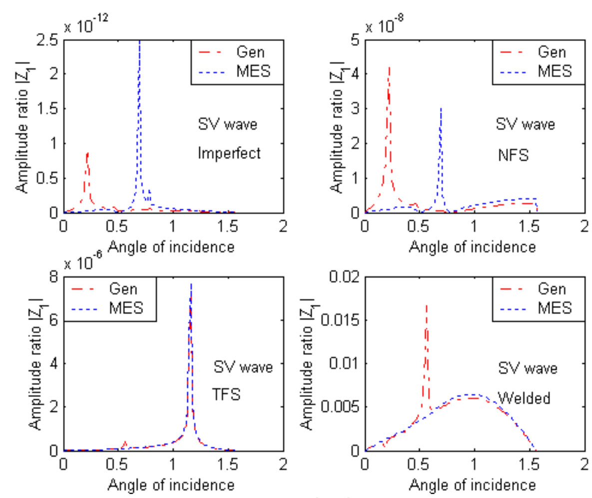

Figure (63)-(66): Variation of the $|Z_1|$ with angle of incidence of the incident transverse wave

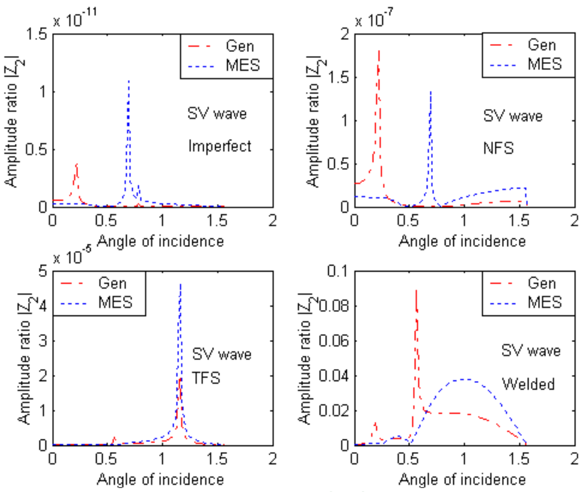

Figure (67)-(70): Variation of the $|Z_2|$ with angle of incidence of the incident transverse wave

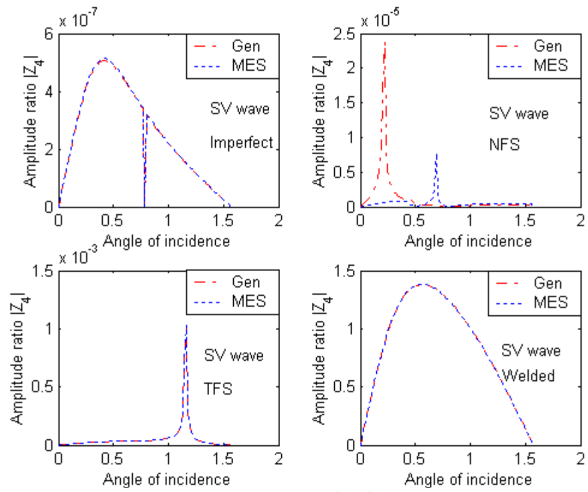

Figure (75)-(78): Variation of the $|Z_4|$ with angle of incidence of the incident transverse wave

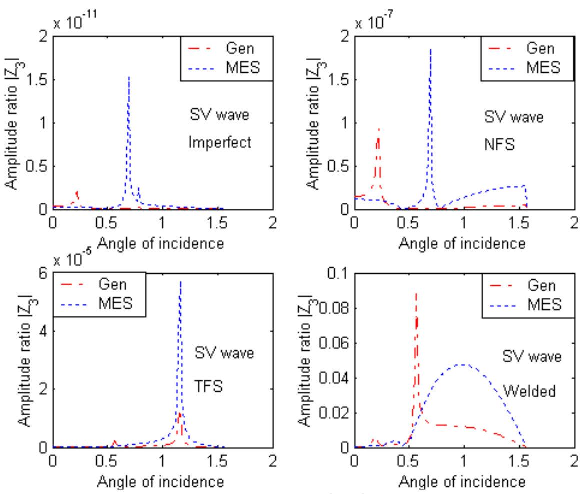

Figure (71)-(74): Variation of the $|Z_3|$ with angle of incidence of the incident transverse wave

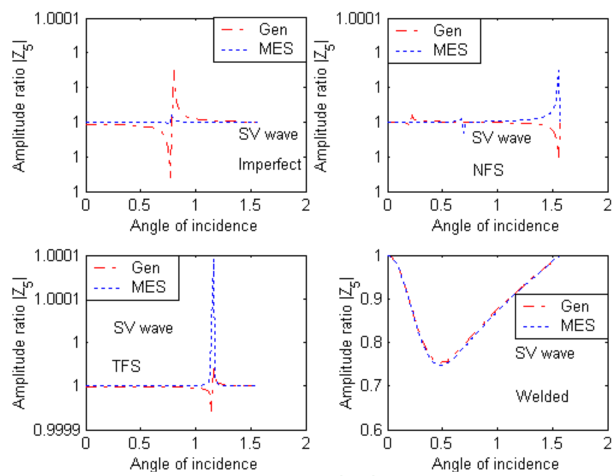

Figure (79)-(81): Variation of the $|Z_5|$ with angle of incidence of the incident transverse wave

CONCLUSION

In conclusion, a mathematical study of reflection and transmission coefficients at an imperfect interface separating micropolar viscoelastic solid half space and fluid saturated incompressible porous half space is made when longitudinal wave or transverse wave is incident. It is observed that

1. The effect of incident wave is significant on amplitude ratios. All the amplitudes ratios are found to depend on incident waves.
2. The velocities of various reflected and transmitted waves are found to be complex valued.
3. The modulus of amplitudes ratios of various reflected and transmitted waves depend on the angle of incidence of the incident wave and material properties of half spaces.
4. The effect of fluid filled in the pores of incompressible fluid saturated porous medium is significant on the amplitudes ratios for reflected and transmitted waves.
5. The effect of stiffness is significant either longitudinal wave is incident or transverse wave is incident.
6. If we neglect the viscous effect of micropolar viscoelastic solid then the variations in the amplitude ratios of various transmitted waves have been affected significantly either longitudinal wave is incident or transverse is incident.
7. Effect of viscosity of micropolar viscoelastic solid is more on modulus of amplitude ratios for transmitted waves.

8. Effect of viscosity is more for transmitted wave than for reflected waves.

Hence the amplitudes ratios of various reflected and transmitted waves depend on material properties and angle of incidence of the incident wave. The model presented in this paper is one of the more realistic forms of the earth models. The present theoretical results may provide useful information for experimental scientists/researchers/seismologists working in the area of wave propagation in micropolar viscoelastic solid/fluid saturated incompressible porous solid.

REFERENCES

1. Bowen, R.M., Incompressible porous media models by use of the theory of mixtures, J. Int. J. Engg. Sci. 18, 1129-1148, 1980.
2. Chen W.Q., Cai J.B., Ye G.R., Wang Y.F., Exact three-dimensional solutions of laminated orthotropic piezoelectric rectangular plates featuring interlaminar bonding imperfections modeled by a general spring layer, International Journal of Solid and Structures, 41, 5247-5263, 2004.
3. De Boer, R. and Didwania, A. K., Two phase flow and capillarity phenomenon in porous solid- A Continuum Thermomechanical Approach, Transport in Porous Media (TIPM), 56, 137-170, 2004.
4. De Boer, R. and Ehlers, W., Uplift, friction and capillarity-three fundamental effects for liquid- saturated porous solids. Int. J. Solid Structures B, 26, 43-57, 1990.
5. De Boer, R. and Ehlers, W., The development of the concept of effective stress, Acta Mechanica A 83, 77-92, 1990.
6. De Boer, R., Ehlers, W. and Liu, Z., One-dimensional transient wave propagation in fluid-saturated incompressible porous media, Archive of Applied Mechanics, 63(1), 59-72, 1993.
7. De Boer, R. and Liu, Z., Plane waves in a semi-infinite fluid saturated porous medium, Transport in Porous Media, 16 (2), 147-173, 1994.
8. De Boer, R. and Liu, Z. ; Propagation of acceleration waves in incompressible liquid – saturated porous solid, Transport in porous Media (TIPM), 21, 163-173, 1995.
9. Eringen, A.C., Linear theory of micropolar viscoelasticity, International Journal of Engineering Science, 5,191-204, 1967.
10. Eringen, A.C. and Suhubi, E.S., Nonlinear theory of simple micro-elastic solids I, International Journal of Engineering Science, 2, 189-203, 1964.
11. Fillunger, P., Der Auftrieb in Talsperren. Osterr. Wochenschrift fur den offen!.Baudienst, Franz Deuticke, Wien, 1913.
12. Gautheir, R.D., Experimental investigations on micropolar media, Mechanics of micropolar media (eds) O Brulin, R K T Hsieh (World Scientific, Singapore), p.395, 1982.
13. Kumar, R., Barak, M., Wave propagation in liquid-saturated porous solid with micropolar elastic skelton at boundary surface, Applied Mathematics and Mechanics, 28(3), 337-349, 2007.
14. Kumar, R, and Chawla, V., Effect of rotation and stiffness on surface wave propagation in elastic layer lying over a gereralized thermodiffusive elastic half-space with imperfect boundary, Journal of solid mechanics, 2(1), 28-42, 2010.
15. Kumar, R. and Hundal, B. S.; Surface wave propagation in fluid – saturated incompressible porous medium, Sadhana, 32(3), 155-166, 2007.
16. Kumar, R., Miglani, A. and Kumar, S., Reflection and Transmission of plane waves between two different fluid saturated porous half spaces, Bull. Pol. Ac., Tech., 227-234, 59(2), 2011.
17. Kumari, N., Wave propagation at liquid/fluid saturated incompressible porous solid interface, International journal of Mathematics Trends and Technology, 11(1), 24-39, 2014.
18. Kumari, N., Reflection and transmission of longitudinal wave at micropolar viscoelastic solid/fluid saturated incompressible porous solid interface, Journal of Solid Mechanics, 6(3), 240-254, 2014.
19. Liu, Z., Propagation and Evolution of Wave Fronts in Two-Phase Porous Media, TIPM, 34, 209-225, 1999.
20. Singh, B., Reflection of plane micropolar viscoelastic waves at a loosely bonded solid-solid interface, Sadhana, 27(5), 493-506, 2002.
21. Suhubi, E.S. and Eringen, A.C., Nonlinear theory of micro-elastic solids II, International Journal of Engineering Science, 2, 389-404, 1964.

Source of Support: None Declared
Conflict of Interest: None Declared